Journal of Rehabilitation in Civil Engineering 7-2 (2019) 86-100

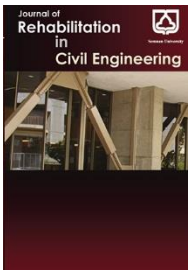

journal homepage: http://civiljournal.semnan.ac.ir/

Seismic Fragility Assessment of Steel SMRF Structures under Various Types of Near and Far Fault Ground Motions

M. Razi[1*], M. Gerami[2], R. Vahdani [3] and F. Farrokhshahi[4]

1. Ph.D. Student of Civil Engineering, Semnan University, Semnan, Iran
2. Associate Prof. of Civil Engineering, Semnan University, Semnan, Iran
3. Assistant Prof. of Civil Engineering, Semnan University, Semnan, Iran
4. M.Sc. Student of Earthquake Engineering, Semnan University, Semnan, Iran

Corresponding author: m.razi@*students.semnan.ac.ir*

ARTICLE INFO

Article history:
Received: 13 April 2017
Accepted: 16 April 2018

Keywords:
Seismic Collapse,
Steel Moment Frame,
Near Fault Ground Motions,
Fragility Analysis,
4th Edition of Standard No. 2800.

ABSTRACT

In this paper, the seismic collapse probability of special steel moment-resisting frame (SSMRF) structures, designed to 4th edition of Iranian seismic design code, under near fault pulse-like and far fault ordinary ground motions is evaluated through fragility analysis. For this purpose, five sample frames with 3 to 15 stories are designed and imposed to the ground motion excitations with different characteristics. Fragility curves are derived for the sample frames using the results of incremental dynamic analyses. Three sets of near fault ground motion records with different range of pulse period and one set of far fault ordinary records are used in dynamic analyses. Each record set involves ten acceleration time histories on soil type III. Based on the obtained results, it was found that pulse-like motions with medium- and long-period pulses are significantly more destructive than other types of ground motions. Fragility analysis reveals that the average collapse probability for the case study frames under the far and near fault ground motions at the intensity of 0.35g equals to 4.3% and 10.3%, respectively. These values are 15.9%and 38.6%, for PGA of 0.53g. It is also found that the increase in the height, leads to increase in higher modes effect to transfer drift demands toward upper stories.

DOI: 10.22075/JRCE.2018.11039.1179

1. Introduction

Constructions located at the near distances to active faults are prone to undergo high-amplitude narrow-band excitations which may impose severe damage to the structural systems. The impulsive character of near fault ground motions, which is mostly due to forward directivity effect, appears in velocity time-history [1]. Velocity pulses form in direction normal to the fault rupture line. Generally, when a large amount of seismic energy dissipates within a few cycles, the formation of plastic hinges may concentrate in a limited number of structural elements [2]. This phenomenon leads to accumulation of damage within the certain parts of structures causing severe outcomes (Lin et al, 2010). Essentially, when the pulse period of near fault ground motions approaches the natural period of the system, the damaging outcomes tends to increase. Sehhati et al (2011)[3] suggested that when the ratio of pulse period to natural period of the structure (T_p/T_n) falls in 0.5-2.5 range, the impulsive feature of the ground motion dominates the seismic response of the system. For medium- to high-rise structures, the higher modes effect may also contribute to the large strength demands in structural elements [4].

Considering the fact that pulse-like records have caused severe damages to multi-story buildings during last major earthquakes (e.g., Northridge 1994, Kobe 1995, Chi Chi 1999 and Bam 2003), it was found that the inclusion of special specifications in seismic design codes to consider damaging potential of near fault ground motions is necessary [5]. Modification of the design spectrum ordinates by modifying factors (N_v and N_a) is a practical approach presented in UBC97 to take account the near fault effects in design of structural systems. This method is similarly adopted by fourth edition of Iranian seismic design code (standard No. 2800). Accordingly, the design spectrum ordinates are multiplied by an amplification factor (N factor), which can be obtained from Eq. (1).

$$\boldsymbol{N = 1 + \frac{N_{max}-1}{4-T_s}(T - T_s); 1 \le N \le N_{max}} \quad (1)$$

Where N_{max} is 1.7 for high and very high seismicity regions and 1.4 for low and medium seismic regions, T_s is 0.7s for soil class III with shear wave velocity of 175-375 m/s and T is the fundamental period of vibration.

This provision predicts that the effect of near fault excitations is more crucial for structures with longer periods. This assumption arises from the fact that the pulse period of near fault ground motions are expected to be in long periods range [6].

It is remarkable that the amplification of elastic response spectrum only considers the influence of pulse-like records on SDOF systems whereas a large portion of damaging potential of such excitations is associated with MDOF and higher-modes effect [7]. The consideration of higher mode effects and nonlinear behaviour characteristics of near fault pulse-like excitations in design process of structures at near fault regions have been the subject of many researches in last decades [8]. For example, the modification of behaviour factor for near fault excitations is one of the approaches proposed by researchers to take account the damaging potential of near fault earthquakes in design of structures [9]. However, it seems more practical to combine the modifications of elastic design spectrum and behaviour factor to a single modification factor called inelastic response spectrum modification.

The fourth edition of Iranian seismic code

has adopted other modifications compared to the previous edition. Accordingly, the lateral load pattern for pseudo-static analysis of structures against seismic loads is defined as follows:

$$F_i = \frac{w_i {h_i}^k}{\sum_{j=1}^{n} w_j {h_j}^k} V \quad (2)$$

Where, k is a function of the fundamental period of oscillation as follows:

$$k = 0.75 + 0.5T \;\; ; \;\; 1 < k < 2 \quad (3)$$

This equation is the same as presented in FEMA 356 [10]and ASCE 7-10 standards for static analysis of the building structures.

In this study, the seismic vulnerability of the steel special moment-resisting frames designed to the fourth edition of Iranian seismic design code under different types of near fault forward directivity records as well as ordinary far fault excitations, is evaluated using the fragility analysis. Moreover, the effect of ground motion type on the pattern of seismic damage distribution along the height of structures is investigated in the last section.

For this purpose, five sample special steel moment-resisting frame (SSMRF) structures (described in section 3) are designed and imposed to four different sets of ten ground motion records. Three sets of the records are near fault pulse-like and the other set consists of ordinary far fault records. The aim of using three different ensembles of near fault records with different range of periods (as described in section 2) is to take account all types of near fault records and obtain the more reliable results. In addition, the influence of pulse period associated with different kinds of earthquake excitations can be evaluated using this method.

The term "collapse" used in this paper, implies to exceedance the prescribed damage levels. Considering the fact that the requirements of capacity design method are satisfied for the sample structures, the damage levels can be represented by inter-story drift limits. Using the results of IDA analyses the fragility curves are developed and used for prediction of seismic vulnerability against future seismic events.

2. Ground Motion Records

Three sets of near fault and one set of ordinary far fault ground motion records each of which including 10 acceleration time histories on soil type III, according to the specifications of Iranian seismic design code (where average shear wave velocity within the depth of 30 m is in 175-375 m/s range), are used in IDA analyses [8].

The far fault ordinary ground motions are recorded at far distances to the fault rupture and lack any impulsive characteristics. The acceleration time histories are downloaded from website of PEER strong motion database. Mean period, T_m, of the far fault ground motions is calculated based on the expression proposed by Rathje et al (2004). The average mean period for far fault records is 0.7s which coincides to corner period suggested by seismic design codes for soil class ***III***. The major specifications of far fault records are provided in Table 1. The magnitude of this set of records is between 6 and 7.6 and the nearest distance to the fault rupture is between 10 and 96 km.

Near fault pulse-like records are selected from those having strong velocity pulses in their time-history, mainly due to forward directivity, as proposed by Soltangharaei et al (2016) [5]. In 2007, Baker proposed three quantitative criteria to identify the forward

directivity records and introduced a sum of 92 records satisfying those criteria. Baker stated that a record is pulse-like only if (1) the velocity pulse appears at the beginning of the record, (2) recorded PGV is larger than 30 cm/s and the pulse index (PI) is larger than 0.85. It is notable that the near fault records selected for this study satisfy the mentioned criteria. In 2014, Shahi and Baker [11]published a paper supported by MATLAB scripts to identify the pulse period of the pulse-like ground motions. This method is employed to measure the T_p for the pulse-like records. It is notable that the downloaded acceleration time history records are oriented to the direction normal to the fault rupture line.

The uncertainty in ground shaking intensity is taken account through incremental scaling of records in IDA analysis. To consider the effect of frequency content, Kumar et al (2013)[12] suggested the acceleration time history records to be classified into three groups of short, medium and long period records. However, the boundaries to define these groups are not clearly identified. In fact, it depends to the parameters such as shaking intensity and structural characteristics. It has been proved that for pulse-like records, the pulse period efficiently characterizes the frequency content characteristics. Therefore, the near fault records are classified into three groups with the same number of records, based on the pulse period range, as follows:

(1) Short-period (SP) records with $t_p < 2s$

(2) Mean-period (MP) records with $2s \leq t_p \leq 4s$

(3) Long-period (LP) records with $t_p > 4s$

The notations mentioned above will be used hereafter to address the record sets. The main goal to employ three different near fault ground motions with different range of pulse period is to compare the influence of near fault records in terms of pulse period and select the most destructive ones as the representative of near fault earthquakes. In other words, the division of pulse-like records into three groups leads to more conservative results. The mean response spectrum for the selected ensembles of records on soil type III, accompanying with design-basis spectrums are provided in Figure 1.

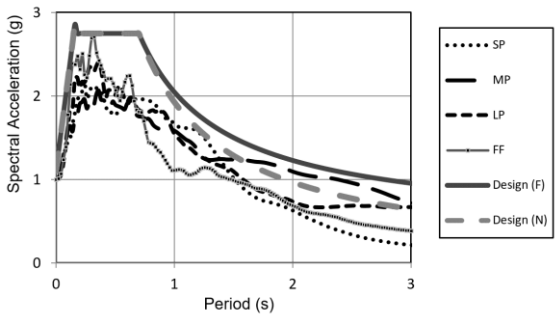

Fig. 1. Acceleration response spectrum of the record ensembles.

In Figure 1, the "Design (F)" case refers to the normalized design spectrum without application of N factor, according to Iranian seismic design code and "Design (N)" case implies to design spectrum for near fault records. The acceleration response spectrum for each record is calculated through solving motion equation for oscillators with different periods and viscous damping ratio of 5%, imposed to the records scaled to gravity acceleration. The mean spectrum for each set of records is obtained by averaging the spectrum ordinates of its records. It is observed that for regular frames with period range of about 0.5-2 seconds, the response spectrum values associated with medium and long period records tend to be larger than other record sets.

Table 1. Far fault ground motion records (FF set).

No	Earthquake	M_W	R (km)	Tm (s)	PGV (cm/s)	RVA (s)
1	Chi-Chi CHY101-W, Taiwan, September 20, 1999	7.6	11.14	1.29	70.64	0.2
2	Imperial Valley, H-E01240, October 15, 1979	6.5	10.4	0.75	31.58	0.1
3	Loma Prieta, G02090, October, 1989	6.9	12.7	0.88	40.21	0.13
4	Loma Prieta, G03090, October 18, 1989	6.9	14.4	0.92	44.72	0.12
5	Northridge, CNP 196, January 17, 1994	6.7	15.8	0.8	60.7	0.15
6	Northridge, LOS000, January 17, 1994	6.7	13	0.7	43.1	0.11
7	Tabas, BOS-T1, September 16, 1978	7.4	26.1	0.77	15.44	0.11
8	Kobe, HIK000, January 16,1995	6.9	95.72	0.9	20.22	0.23
9	N. Palm Springs, TFS000, July 8, 1986	6.06	64.8	0.37	6.9	0.06
10	Manjil 1990, BHRC Rudsar	7.37	64.67	0.69	11.54	0.12

The main characteristics of three sets of near fault ground motion records are presented in Table 2.

Table 2. Near fault pulse-like records.

Short-period records (Tp < 2s)							
No	Earthquake	M_W	R (km)	Tp (s)	Tm (s)	PGV (cm/s)	RVA (s)
1	1983 Coalinga-05, Oil City	5.8	8.46	0.7	0.47	41	0.05
2	1986 Taiwan SMART1(40), SMART1 M07	6.3	4.04	1.6	1.17	36	0.16
3	1986 N. Palm Springs, North Palm Springs	6.1	4.04	1.4	0.76	74	0.11
4	1987 Whittier Narrows-01, Downey - Co Maint Bldg	6	20.82	0.8	0.7	30	0.13
5	1987 Whittier Narrows-01, LB - Orange Ave	6	24.54	1	0.69	33	0.13
6	1989 Loma Prieta, Gilroy Array #2	6.9	11.07	1.7	0.79	46	0.11
7	2004 Parkfield 02-CA, Fault Zone 9	6	2.85	1.13	0.91	24	0.16
8	1995 Kobe, Japan, Takarazuka	6.9	0.27	1	0.9	73	0.11
9	1995 Kobe, Japan, Takatori	6.9	1.47	1.6	1.28	170	0.25
10	1997 Northwest China-03, Jiashi	6.1	17.73	1.3	0.67	37	0.14
Medium-period records (2s < Tp < 4s)							
1	1979 Imperial Valley-06, El Centro, Array #3	6.5	0.34	2.4	0.92	44	0.13
2	1979 Imperial Valley-06, El Centro Array #6	6.5	1.35	3.8	1.69	112	0.26
3	1980 Irpinia, Italy-01, Sturno	6.9	10.48	3.1	1.21	*41*	0.19
4	1981 Westmorland, Parachute Test Site	5.9	16.66	3.6	0.91	36	0.21
5	1987 Superstition Hills-02, Parachute Test Site	6.5	0.95	2.3	1.17	107	0.26
6	1989 Loma Prieta, Alameda Naval Air Stn Hanger	6.9	71	2	1.07	32	0.15
7	1992 Erzincan, Turkey, Erzincan	6.7	4.58	2.72	1.55	95	0.2
8	1992 Cape Mendocino, Petrolia	7	8.18	3	0.75	82	0.14
9	1994 Northridge-01, Jensen Filter Plant	6.7	5.43	3.5	1.07	67	0.13
10	1994 Northridge-01, Newhall - W Pico Canyon Rd	6.7	5.48	2.4	1.63	88	0.21
Long-period records (Tp > 4s)							
1	1979 Imperial Valley-06, EC County Center FF	6.5	7.31	4.5	1.33	54	0.31
2	1979 Imperial Valley-06, El Centro Array #11	6.5	12.45	7.4	0.55	41	0.11
3	1979 Imperial Valley-06, El Centro Array #7	6.5	0.56	4.2	1.37	109	0.24
4	1979 Imperial Valley-06, El Centro Differential Array	6.5	5.09	5.9	0.77	60	0.15
5	1979 Imperial Valley-06, Holtville Post Office	6.5	7.65	4.8	0.81	55	0.22
6	1989 Loma Prieta, Saratoga - Aloha Ave	6.9	8.5	4.5	0.96	56	0.16
7	1992 Landers, Yermo Fire Station	7.3	23.62	7.5	0.96	53	0.24
8	1999 Chi-Chi, Taiwan, CHY101	7.6	9.96	4.8	1.07	85	0.19
9	1999 Chi-Chi, Taiwan, TCU101	7.6	2.13	10	0.87	68	0.33
10	1999 Chi-Chi, Taiwan, TCU136	7.6	8.29	10	0.99	52	0.31

3. Sample Structures

Five steel special moment-resisting frames (SSMRFs) involving 3, 6, 9, 12 and 15 stories on soil type III and at high-seismicity regions, with analytical periods of 0.85, 1.24, 1.52, 1.72 and 1.98 seconds are selected as sample structures. The story height and bay width for all frames are 3.2m and 6.0m, respectively. Configuration of the sample frames is depicted in Figure 2.

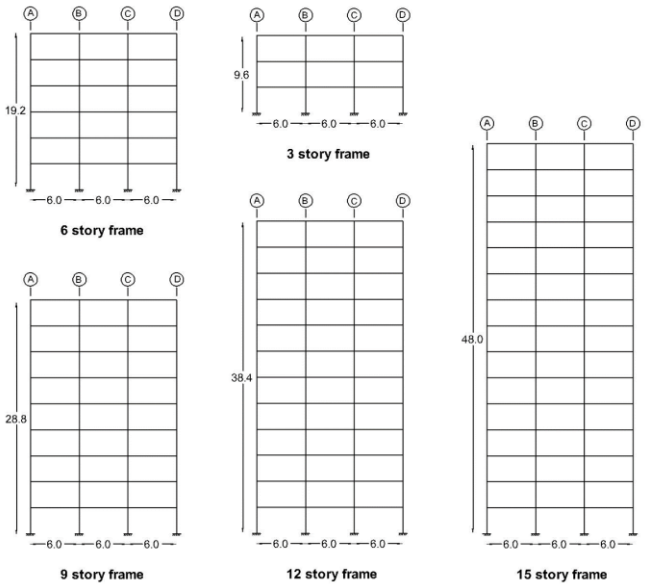

Fig. 2. Configuration of the sample moment frame.

Dead load of 1250 kg/m and live load of 375 kg/m are applied to beam elements at all floors. Seismic mass of 50 ton is assigned to all floor levels which are added to structural members weight. Seismic loading of the structures are implemented in compliance with specifications of Iranian seismic design code. Accordingly, the peak ground acceleration for structures located at high-seismicity regions is 0.35g. The structural design of the frames satisfies the requirements of Iranian standard for design of steel structures.

Static analysis and design of the frames are performed using the ETABS software. The design sections for case study frames are provided in Table 3.

Table 3. Design sections for sample frames

Frame	story	Columns in axes A , D	Columns in axes B , C	Beams
15 story	1-3	Box 360x360x28	Box 400x400x30	IPE 550
	4-6	Box 320x320x25	Box 360x360x28	IPE 550
	7-10	Box 280x280x20	Box 340x340x25	IPE 550
	11	Box 260x260x2	Box 340x340x25	IPE 500
	12-13	Box 240x240x20	Box 320x320x20	IPE 450
	14-15	Box 220x220x14.5	Box 240x240x16	IPE 360
12 story	1-3	Box 320x320x25	Box 380x380x28	IPE 500
	4-5	Box 280x280x25	Box 340x340x28	IPE 500
	6	Box 280x280x25	Box 340x340x28	IPE 450
	7-8	Box 260x260x25	Box 320x320x25	IPE 450
	9	Box 240x240x16	Box 280x280x20	IPE 450
	10	Box 240x240x16	Box 280x280x20	IPE 400
	11-12	Box 220x220x12.5	Box 240x240x14	IPE 360
9 story	1-3	Box 300x300x25	Box 360x360x25	IPE 450
	4-5	Box 260x260x25	Box 320x320x25	IPE 450
	6-7	Box 240x240x20	Box 300x300x25	IPE 400
	8-9	Box 220x220x12.5	Box 240x240x12.5	IPE 360
6 story	1-2	Box 280x280x22	Box 320x320x22	IPE 400
	3-4	Box 260x260x20	Box 300x300x20	IPE 400
	5-6	Box 220x220x14	Box 240x240x20	IPE 360
3 story	1-3	Box 220x220x12	Box 240x240x16	IPE360

The Seismostruct software version 7.4.0 [13] is utilized for implementation of incremental dynamic analyses. This software is specialized for analysis of frame structures under seismic loads. The nonlinear behaviour of structural members can be modelled using either by fiber-based or concentrated plasticity elements. In this study, fiber-based hinges formulated by Scott and Fenvese (2006)[14] are used to model beam and column elements. This modeling technique has been widely used and recognized as an standard tool for seismic assessment studies [5]. This type of fiber-based element accommodates the distribution of inelasticity within a predefined fraction of the member length at two ends. This ratio is assumed to be 15%. The most important advantage for using fiber-based elements is the accurate modelling of interaction between axial force and bending moments within frame elements. Beams and columns sections are divided into 200 fibers to ensure the preciseness of the analysis. The steel grade St-37 with elasticity modulus of 210 GPA and yield stress of 240 MPA is used as structural material. Material nonlinear behaviour is modelled using a bilinear stress-strain curve with 3% strain-hardening ratio. Beam-to-column connections are assumed to be fully rigid. The geometric nonlinearity is included in analysis algorithms. In time-history analyses, Rayleigh damping is assumed 2% for first mode and 5% for second mode of vibration [7]. The columns are fixed to the ground at the base level and the torsion failure modes are ignored.

4. Fragility Analysis

Fragility curves check if the predefined performance levels are satisfied under different levels of ground motion excitations. The fragility curves can be used in retrofitting decisions, estimating of casualties and economic losses and finally the disaster planning problems. Fragility functions can be generated using the data collected from various methods including field observations, engineering judgment and structural analysis [15-17]. Here, the fragility curves are developed using the results of structural analysis where the intensity of ground motions and the number of analyses can be controlled by analyst. There are numerous analytical approaches to collect the required data for fragility analysis, from which the incremental dynamic analysis (IDA) proposed by Cornell and Vamvatsikos (2002) [18] is one of the most efficient and reliable methods. In this method, a suite of ground motion records are increasingly scaled to find the intensity at which L.S. conditions are not satisfied. This approach is widely utilized for developing fragility curves [19,5]. In order to establish the fragility curves the ground motion intensity and damage states must be quantitatively represented by intensity and damage measures, respectively. For the purpose of the current research, peak, ground acceleration (PGA) is selected as intensity measure. The damage states (or performance levels) are commonly interpreted in terms of inter-story drift ratio. Although the story drift ratio may not precisely represent the damage state of the structure, it is commonly used as an efficient and practical measure for quantification of performance levels (FEMA 356)[9]. According to the specifications of Iranian seismic design code for moment-resisting frame structures, the inter-story drift ratio at any floor level must not exceed 2.0%, for structures with more than 5 stories and 2.5%, for lower buildings. These thresholds are considered as the collapse points for the sample frames.

A statistical distribution function must be fitted on the data. Through a large number of observations, It has been proved that the log-normal cumulative distribution function often has a suitable fit on the fragility function data [20]. Hence, the fragility function is expressed as:

$$P(C|IM = im) = \Phi\left(\frac{Ln(im/\Theta)}{\beta}\right) \quad (4)$$

Where, $P(C|IM = im)$ is the probability of collapse or exceeding a performance criteria under a seismic load with intensity of im, $\Phi(\,)$ is the standard normal cumulative distribution function (CDF), θ is the median of fragility function (the IM corresponding to 50% probability of collapse), and β is the standard deviation of ln (IM).

This expression implies that the IM values corresponding to occurrence of collapse is log-normally distributed.

The fitting method proposed by Baker (2015) [21] which is based on moment method is used for plotting fragility curves with log-normal cumulative distribution function. The mean and standard deviation (Ln(θ),β) for distribution function of ln(IM) values are computed using equations 5 and 6.

$$\ln(\theta) = \frac{1}{n}\sum_{i=1}^{n}\ln(IM_i) \quad (5)$$

$$\beta = \sqrt{\frac{1}{n-1}\sum_{i=1}^{n}\ln(IM_i/\theta)} \quad (6)$$

In above expressions, n is the number of ground motion records and IM_i is the intensity of ith ground motion corresponding to onset of collapse for the given structure.

Employing this procedure, the fragility curves are drawn for case study frames under the four sets of ground motions. These curves are used to estimate the vulnerability of the sample structures against seismic loads with different characteristics.

5. Results and Discussion

Incremental dynamic analyses were conducted to find the IM values corresponding to the predefined drift limits. The results of IDA analyses for the 15story frame are presented in Figure 3. The intensity of ground motions is represented by PGA to facilitate the comparison between different ground motions with the same amplitudes. The dispersion of IDA curves in each sheet indicates that the effect of time duration and frequency content is considerable, even if the records belong to the same soil type.

The mean IDA curves associated with each set of records for the case study frames is derived by averaging the IDA curves for those records. The resultant mean IDA curves are provided in Figure 4. It is observed that with increase in the height, the PGA values corresponding to the same drift values tend to grow. In other words, the higher structures will undergo less damage when imposed to the same seismic loads. This is due to the fact that larger frames have higher degree of redundancy resulting larger seismic capacity. In addition, the design code specifications are more stringent for taller constructions.

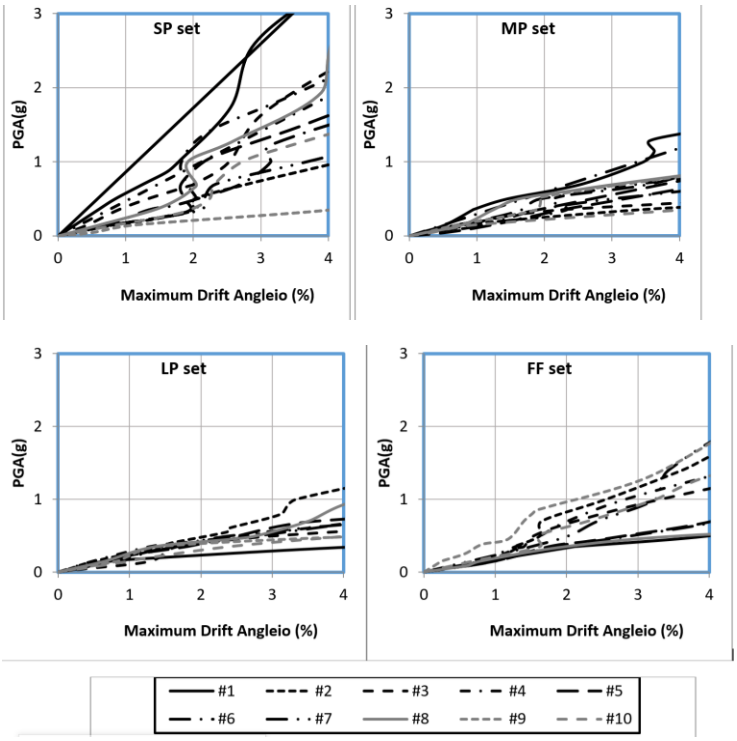

Fig. 3. IDA curves for 15story frame.

For example, the N factor computed from Eq. (1), is 1.0 for 3story frame and reaches the 1.24 for 15story frame. Consequently, the more conservative specifications lead to lower seismic vulnerability for tall structures. Moreover, the difference among the IDA curves associated with different record sets is more tangible for higher frames. This is mainly due to the effect of higher modes which is more crucial for structures with more degree of freedom. Soltangharaei et. al. (2016) [5]presented similar curves for 10 story model with PGA range of 0.5 to 1.5 for 4% of MIDR, close to 9 story curves of Figure 4.

To compare the damaging strength of the pulse-like ground motion sets with far fault excitations, the ratio of mean PGA equivalent to the prescribed MIDRs[1] for far fault ground motions (IM_{far}) to that of each near fault record sets is calculated for the sample structures. This parameter is denoted by IM ratio (IMR).The IMR values are provided in Figure 5. It is observed that IMR is essentially between 1 and 2.5. This means that far fault ground motions require up to 2.5 times larger PGA to induce the same drift demands to the steel moment frames.

In other words, mid and long period records with PGA of 40% less than far fault motions may induce the same damage level (1/2.5=0.4). However, it depends to the case study and ground motion characteristics. As the height of frames rises up, the effect of long period records gets more severe and the effect of short-period records decrease. Almost in all cases, the MP records tend to impose larger demands to the regular steel moment frames.

[1] Maximum interstory drift ratio

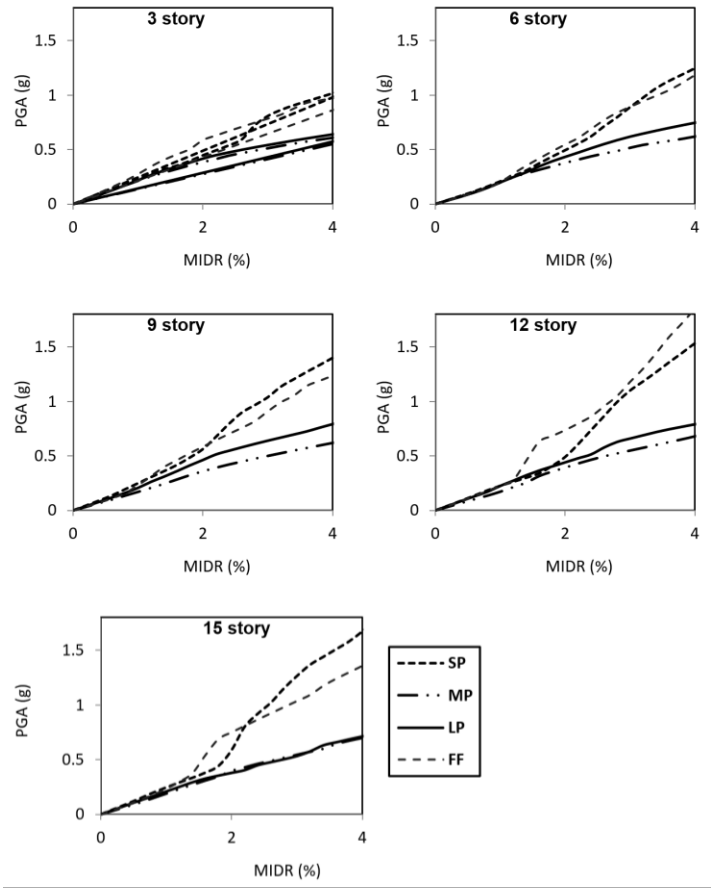

Fig. 4. Mean IDA curves for the sample steel structures.

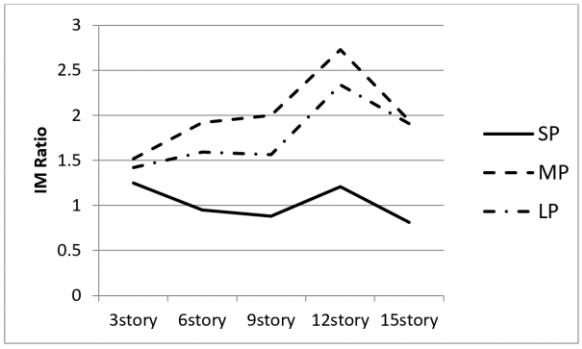

Fig. 5. IM ratios for the sample frames

5.1. Fragility curves

Given the IM values equivalent to predefined MIDR thresholds obtained from IDA analyses, the fragility curves are developed for the sample frames. Fragility curves are provided for each sample frame are illustrated in Figure 6.

Considering the maximum of collapse probability for the three sets of near fault ground motion sets as the representative of vulnerability against near fault ground motions, it is concluded that the collapse probability for the SSMRF structures designed in compliance with Iranian seismic design code against DBE events (PGA=0.35g) is 4.3% for far fault and 10.3% for near fault ground motions. These values change to 15.9% and 38.6% for MCE hazard level (assuming PGA of $1.5 \times 0.35\text{g} = 0.525\text{g}$). The collapse probability for 3story frame seems to be larger compared to taller structures. This is due to more conservative specifications for design of structures with more than 5 stories.

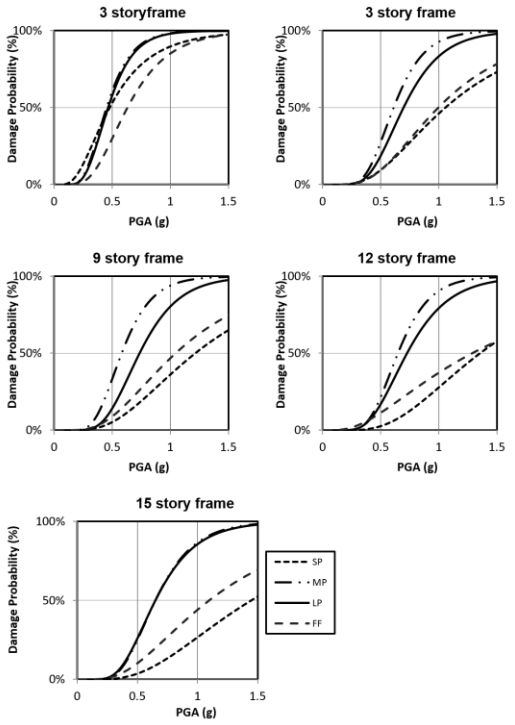

Fig. 6. Fragility curves for the sample structures.

Using the data obtained from fragility curves, the collapse probability equivalent to MCE hazard level is derived for the steel frames, as illustrated in Figure 7. It has been proved that long period pulse-like motions are more destructive than short period excitations. However, the difference might be nontangible for shorter frames since the period of such structures is close to the short period range with reduce this difference.

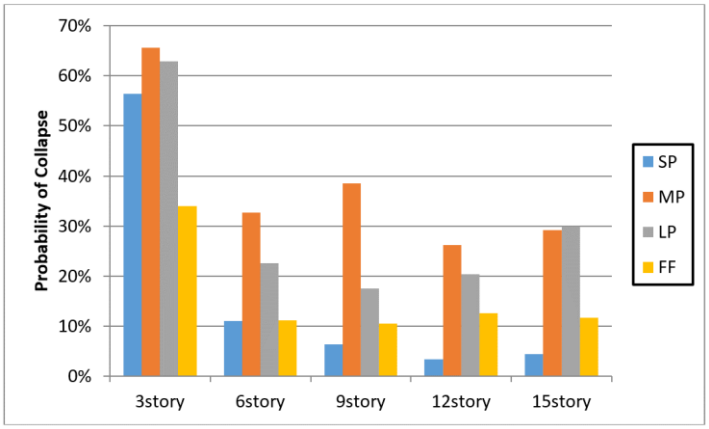

Fig. 7. Probability of collapse in PGA of 0.525g.

To examine the efficiency of the spectrum amplification by N factor (Eq. 1) to predict the damaging effects of near fault excitations, the collapse probability for PGA of 0.53g for near fault records is compared with that of far fault records at the PGA of $0.53g \times N$ (amplified intensity), as presented in Table 4. Error values presents the relative difference between the collapse probability obtained from fragility analysis for near fault records

with the collapse probability of far fault records with intensity of N*0.35g (amplified intensity). It is concluded that the near fault records has more severe effects than what N factor predicts. This is more crucial for low-rise structures where the N factor takes values near to unity. One of the main reasons for this bias is that the short-period records may impose larger impacts on low-rise frames. In other words, the near fault effects are not limited to long-period pulse-like records but rather all types of near fault excitations must be considered when evaluating the seismic performance of various structural systems to near fault excitations.

Table 4. Collapse probability for near fault and amplified far fault ground motions, for MCE hazard level (PGA=0.53g).

Frame	N factor	Collapse Probability (%)		
		Near Fault records	Amplified F.F.	Error (%)
3story	1.0	65.7	34.0	94.0
6story	1.05	32.7	13.0	151
9story	1.12	38.5	14.7	162
12story	1.18	26.2	17.5	49.7
15story	1.24	30.0	20.0	50.5

5.2 Damage distribution

In addition to the probability of global collapse, the pattern of seismic damage distribution over the height of the frames is a key parameter to be considered in seismic evaluation and design of structural systems. According to the last researches, the pattern of drift distribution, as an efficient damage index, is highly dependent to the ground motion characteristics (e.g., intensity and frequency content) and structural properties (e.g., structural system, period of vibration, height and geometrical properties) [22]. In this subsection, the distribution of peak story drifts equivalent to prescribed MIDR values is presented in Figure 8.

For low- to mid-rise frames, the drift distribution pattern have a little dependency to the ground motion frequency content, as the peak drifts accumulate in lower parts of the structures. However, for higher frames, the higher modes tend to influence the damage distribution pattern. For example, the short-period records tend to transfer drifts to upper levels whereas the long period records tend to impose larger drifts on lower stories. It should also be noted that the drift distribution depends on the ground motion intensity, as for higher nonlinearity degrees the accumulation of drift demands moves toward lower stories, for all type of seismic excitations.

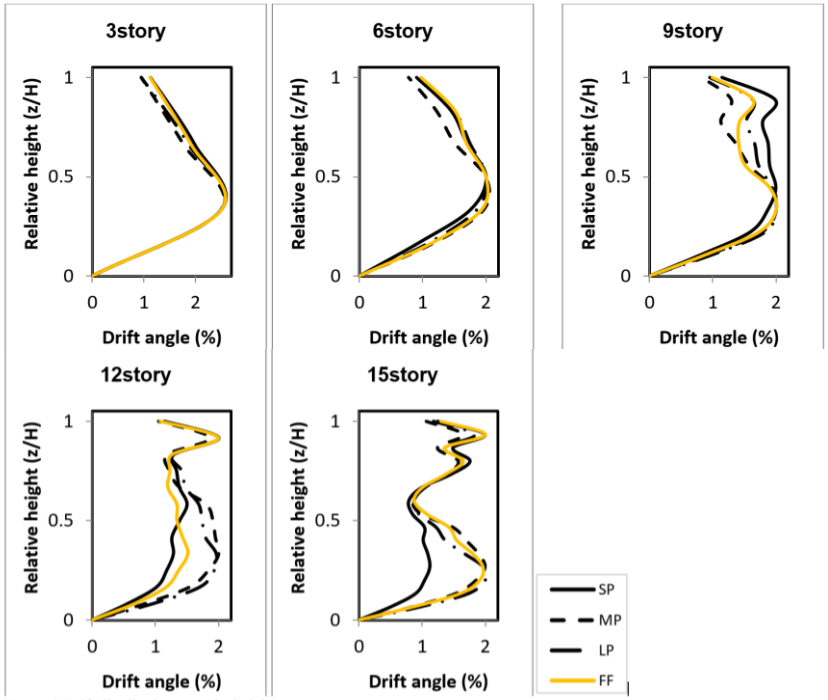

Fig. 8. Drift distribution over the height.

6. Conclusions

The damage probability of the steel special moment-resisting frames designed to 4th edition of Iranian seismic design code under far fault and near fault ground motions was investigated through fragility analysis of the five sample frames with 3 to 15 stories. The IDA analysis approach was employed to derive the intensities equivalent to the exceedance of prescribed drift limits. Three sets of near fault and one set of far fault records were used in this study. In the last part of the research, the seismic damage distribution over the height of the sample frames also was evaluated. The main achievements of the research are summarized as follows:

1) The damaging potential of near fault ground motions is not completely captured by the modification of design spectrum as suggested by Iranian seismic design code and other similar standards.

2) The near fault effects depend on the pulse period of the record. Accordingly, for low-rise structures, the short-period pulse-like excitations may impose larger demands while for larger structures the mid- and long-period records induce more severe damage.

3) The average collapse probability for the regular SSMRF structures designed to the 4th edition of Iranian seismic design code against near and far fault ground motions at the PGA of 0.35g, equals to10.3% and4.3%, respectively. Assuming a PGA of 0.53g for MCE hazard level, the mentioned probabilities change to 38.6% and 15.9%.

4) The collapse probability tends to decrease for taller structures which have ***bigger*** redundancy degree. However, the design specifications (including spectrum

amplification coefficient) is more conservative for taller structures.

5) The pattern of drift distribution over the height of the frames depends to the frequency content of the ground motion records, specifically for high-rise frames. Short-period records tend to transfer drifts toward upper stories while the mid- and long-period records induce larger drifts at lower parts of the structures.

REFERENCES

[1] Shome, N., Cornell, C.A., Bazzurro, P. and Carballo, J.E. (1998). "Earthquakes, records, and nonlinear responses". Earthquake Spectra, Vol. 14, No. 3, pp.469-500.

[2] Khashaee, P., Mohraz, B., Sadek, F., Lew, H.S., Gross, JL, (2003). "Distribution of earthquake input energy in structures". Research report No. NISTIR 6903. National Institute of Standards and Technology, Gaithersburg, USA.

[3] Sehhati, R., Rodriguez-Marek, A., ElGawady, M., William, F. (2011). "Effects of near-fault ground motions and equivalent pulses on multi-story structures". Engineering Structures, Vol. 33, pp. 767–779.

[4] Soleimani Amiri, F., GhodratiAmiri, G., Razeghi, H. (2013). "Estimation of seismic demands of steel frames subjected to near-fault earthquakes having forward directivity and comparing with pushover analysis results". Struct. Design of Tall Spec. Build, Vol. 22, pp. 975–988.

[5] Soltangharaei, V., Razi, M., Vahdani, R. (2016). "Seismic fragility of lateral force resisting systems under near and far-fault ground motions". International journal of structural engineering, Vol. 7, No. 3, pp. 291-303.

[6] Somerville, P. (2005). "Engineering Characterization of near-fault ground motions". NZSEE Conference, Planning and Engineering for Performance in Earthquake, Taupo, New Zealand.

[7] Gerami, M., Abdollahzadeh, D. (2015). "Vulnerability of steel moment-resisting frames under effects of forward directivity". Struct. Design Tall Spec, Vol. 24, pp. 97–122.

[8] Razi, Morteza, Mohsen Gerami, and Reza Vahdani. "Shear Demands of Steel Moment-Resisting Frames Under Near-and Far-Fault Seismic Excitations." Iranian Journal of Science and Technology, Transactions of Civil Engineering, 1-16, 2017.

[9] Gillie, J.M., Rodriguez-Marek, A., McDaniel, C. (2010). "Strength reduction factors for near-fault forward-directivity ground motions". Engineering Structures, Vol. 32, pp. 273–285.

[10] Federal Emergency Management Agency. FEMA.356. "Prestandard and Commentary for the Seismic Rehabilitation of Buildings", Reston, Virginia, USA.

[11] Shahi, S.K. and Baker, J.W. (2014). "An efficient algorithm to identify strong velocity pulses in multi-component ground motions". Bulletin of the Seismological Society of America, Vol. 104, No. 5, pp. 2456–2466.

[12] Kumar, M., Stafford, P.J., Elghazouli, A.Y. (2013). "Seismic shear demands in multi-storey steel frames designed to Eurocode 8". Engineering Structures,Vol. 52, pp. 69–87.

[13] SeismoStruct. 2015. A computer program for static and dynamic analysis for framed structures. Version 7.0.4, Available from URL:www.seismosoft.com(online).

[14] Scott, M.H. smf Fenvese, G.L. (2006). "Plastic hinge integration method for force-based beam-column elements". ASCE Journal of Structural Engineering, Vol. 132, No. 2, pp. 244-252.

[15] Calvi, G.M., Pinho, R., Magenes, G., Bommer, J. (2006). "Development of seismic vulnerability assessment methodologies over the past 30 years". ISET journal of Earthquake Technology, Vo. 43, No. 3, pp. 75–104.

[16] Kim, S.H. and Shinozuka, M. (2004). "Development of fragility curves of

bridges retrofittedby column jacketing". Probabilistic Engineering Mechanics, Vol. 19, No. 1, pp. 105–112/ 2004.

[17] Shafei, B., Zareian, F., and Lignos, D.G. (2011). "A simplified method for collapse capacity assessment of moment-resisting frame and shear wall structural systems". Engineering Structures, Vol. 33, No. 4, pp. 1107–1116.

[18] Vamvatsikos, D. and Cornell, C.A. (2002). "Incremental dynamic analysis". Earthquake Engineering &

[19] Ibrahim, Y.E. and El-Shami, M.M. (2011). "Seismic fragility curves for mid-rise reinforced concrete frames in Kingdom of Saudi Arabia". The IES Journal Part A: Civil & Structural Engineering, Vol. 4, No. 4, pp. 213-223.

[20] Eads, L., Miranda, E., Krawinkler, H., Lignos, D. G. (2013). "An efficient method forestimating the collapse risk of structures in seismic regions". Earthquake Engineering& Structural Dynamics", Vol. 42, No. 1, pp. 25–41.

[21] Baker, J.W. (2015). "Efficient analytical fragility function fitting using dynamic structural analysis". Earthquake Spectra, Vol. 31, No. 1, pp. 579-599.

[22] Gerami, Mohsen, and Abbas Sivandi-Pour. "Performance-based seismic rehabilitation of existing steel eccentric braced buildings in near fault ground motions." The Structural Design of Tall and Special Buildings 23.12 881-896, 2014.